Study on Treatment with Respect to Idiopathic Scoliosis*
(Sensitivity Analysis Based on Buckling Theory)

Kenzen TAKEUCHI**, Hideyuki AZEGAMI***, Shunji MURACHI****, Junzoh KITOH†, Yoshito ISHIDA††, Noriaki KAWAKAMI††† and Mitsunori MAKINO††††

A hypothesis that the thoracic idiopathic scoliosis is buckling phenomenon of the fourth mode induced by the growth of thoracic vertebral bodies was presented in the previous work by the authors using numerical simulations with finite element model of the spine. If the hypothesis is acceptable, sensitivity function with respect to the critical growth of thoracic vertebrae on the maximization problem of buckling load with the fourth buckling mode gives us useful information to improve and develop treatments for the idiopathic scoliosis. The numerical results analyzed by the finite element method demonstrated that the sensitivity function is high at the articular capsules of the intervertebral joints, the intervertebral disks, the costotransverse joints and the costovertebral joints around the apex of the curvature in the case of the thoracic idiopathic scoliosis.

Key Words: Biomechanics, Computer Aided Analysis, Finite Element Method, Sensitivity Analysis, Idiopathic Scoliosis, Buckling

* Received 11th May, 2001

** Doctoral Course of Mechanical and Structural System Engineering, Graduate School, Toyohashi University of Technology, 1-1 Hibarigaoka, Tempaku-cho, Toyohashi-shi, Aichi 441-8580, Japan. E-mail: takeuchi@az.mech.tut.ac.jp

*** Department of Mechanical Engineering, Toyohashi University of Technology, 1-1 Hibarigaoka, Tempaku-cho, Toyohashi-shi, Aichi 441-8580, Japan. E-mail: azegami@mech.tut.ac.jp

**** Japanese Red Cross Aich Junior College of Nursing, 3-35 Michishita-cho, Nakamura-ku, Nagoya-shi, Aichi 453-0046, Japan

† Emer. Prof. of Nagoya University, School of Medicine, 65 Tsurumai-cho, Showa-ku, Nagoya-shi, Aichi 466-8550, Japan. E-mail: jkitoh@med.nagoya-u.ac.jp

†† Ishida Orthopaedic Surgery, 90-1 Sadamatsu, Takao, Huyou-cho, Tanba-gun, Aichi 480-0102, Japan. E-mail: iy01-ioc@na.rim.or.jp

††† Meijyo Hospital, Orthopaedic Surgery, 1-3-1 Sannomaru, Naka-ku, Nagoya-shi, Aichi 460-0001, Japan. E-mail: nori-aki@pop12.odn.ne.jp

†††† Toyota Memorial Hospital, Orthopaedic Surgery, 1-1 Heiwa-cho, Toyota-shi, Aichi 471-0821, Japan. E-mail: m_makino@mail.toyota.co.jp

1. Introduction

Idiopathic scoliosis is known as a spinal irregularity with lateral curvatures that appear during adolescence, especially the growth spurt, without any remarkable abnormality of the vertebrae or associated musculoskeletal condition. A typical case has an apex of the lateral curvature in thoracic region and is called the thoracic idiopathic scoliosis. In cases that the brace treatments are insufficient, operative fixing treatments are performed to correct the curvature and prevent the progression. Growth arresting occurs by the spine fixing operation, so it is desired to develop more effective treatment using minimum fixation.

With respect to mechanical etiology of the idiopathic scoliosis, a large number of hypotheses have been presented. In the previous work, the authors[1] reviewed them and presented a hypothesis based on the numerical simulation with finite element model of the spine that the thoracic idiopathic scoliosis is a buckling phenomenon of the fourth mode induced by the growth of thoracic vertebral bodies.

If the hypothesis is acceptable, to find the most

sensitive parts to maximize the critical growth generating the fourth buckling mode gives us useful information to improve and develop treatments for the idiopathic scoliosis.

Meanwhile, one of the authors[2)-5)] proposed a solution of structural optimization problems to determine boundary shapes of linear elastic continua that minimize deformation by external forces and maximize buckling load, or the like. With this solution, boundary shape is modified with sensitivity function that is defined by the variational ratio of objective functional with respect to variation of each point on boundary in the outward normal direction. The sensitivity function can be calculated using optimality conditions derived theoretically.

This paper presents the outline of the theory on the maximization problem of the critical growth of thoracic vertebrae and the numerical result with respect to the fourth buckling mode. If the fourth buckling hypothesis is acceptable, these results denote that the high parts in the sensitivity function indicate significant parts to correct the curvature and prevent the progression of the thoracic idiopathic scoliosis.

2. Shape Optimization Problem with Respect to Buckling

The shape optimization theory of linear elastic continua with respect to buckling was presented in the previous paper by one of the authors[5)]. In this section, the theory is modified with initial strain problem.

2.1 Formulation of domain variation

Let us consider that a linear elastic continuum defined on a three dimensional bounded domain $\Omega \subset \boldsymbol{R}^3$, and its boundary Γ, varies to a three dimensional bounded domain $\Omega_s \subset \boldsymbol{R}^3$. This domain variation can be described with a one parameter family of continuous mappings $T_s(X)$: $\Omega \ni X \mapsto x \in \Omega_s$, where s is a parameter to express domain variation history.

2.2 Formulation of buckling loading factor maximization problem

When the growth is given by the bulk strain as used in the previous paper[1)], maximization problem of the critical growth with respect to the domain variation is formulated by the following equations.

$$\min_{\Omega \subset \boldsymbol{R}^3} -\zeta \quad \text{such that} \tag{1}$$

$$a(u^{(0)}, v^{(0)}) = a_\varepsilon(\varepsilon^B, v^{(0)}) \quad u^{(0)} \in U \quad \forall v^{(0)} \in U \tag{2}$$

$$a(u, v) = -\zeta d(u^{(0)}, u, v) \quad u \in U \quad \forall v \in U \tag{3}$$

where the bilinear forms $a(\cdot, \cdot)$, $a_\varepsilon(\cdot, \cdot)$, and the trilinear form $d(\cdot, \cdot, \cdot)$ are defined by

$$a(u, v) \equiv \int_\Omega C_{ijkl} u_{k,l} v_{i,j} dx \tag{4}$$

$$a_\varepsilon(\varepsilon^B, v) \equiv \int_\Omega C_{ijkl} \varepsilon^B_{kl} v_{i,j} dx \tag{5}$$

$$d(u^{(0)}, u, v) \equiv \int_\Omega C_{ijkl} u^{(0)}_{k,l} u_{m,i} v_{m,j} dx \tag{6}$$

Equation (2) denotes the variational form to determine the prebuckling displacement $u^{(0)} = \{u_i^{(0)}\}_{i=1,2,3}$ due to the generation of the bulk strain $\varepsilon^B = \{\varepsilon^B_{ij}\}_{i,j=1,2,3}$ using the virtual, or adjoint, displacement vector $v^{(0)} = \{v_i^{(0)}\}_{i=1,2,3}$. Equation (3) denotes the variational form of the eigen-equation for the buckling loading factor ζ and the buckling mode $u = \{u_i\}_{i=1,2,3}$ using the virtual, or adjoint, displacement vector $v = \{v_i\}_{i=1,2,3}$. The notation U denote admissible set of the displacements satisfying boundary conditions. The tensor $\{C_{ijkl}\}_{i,j,k,l=1,2,3}$ denotes the Hooke stiffness. In this paper, tensor notation with subscripts, the Einstein summation convention and the gradient notation $(\cdot)_{,i} = \partial(\cdot)/\partial x_i$, $x = \{x_i\}_{i=1,2,3} \in \boldsymbol{R}^3$, are used.

Applying the Lagrange multiplier method, or the adjoint method, and the formula of the material derivative, the optimization problem is rewritten by the stationary problem of the Lagrange functional $L(u, v, u^{(0)}, v^{(0)})$ defined by

$$L = -\zeta - a(u, v) - \zeta d(u^{(0)}, u, v) + a(u^{(0)}, v^{(0)}) - a_\varepsilon(\varepsilon^B, v^{(0)}) \tag{7}$$

where $v = \{v_i\}_{i=1,2,3}$ and $v^{(0)} = \{v_i^{(0)}\}_{i=1,2,3}$ were introduced as the Lagrange multipliers, or adjoint variables.

The derivative $\dot{L}(u, v, u^{(0)}, v^{(0)})$ with respect to s is derived using the velocity function $V(x) = \partial T_s(X)/\partial s = \partial T_s(T_s^{-1}(x))/\partial s$, $X \in \Omega$, $x \in \Omega_s$, as follows.

$$\dot{L} = -\dot{\zeta} - a(u', v) - a(u, v') - \dot{\zeta} d(u^{(0)}, u, v) - \zeta d(u^{(0)\prime}, u, v) - \zeta d(u^{(0)}, u', v) - \zeta d(u^{(0)}, u, v') + a(u^{(0)\prime}, v^{(0)}) + a(u^{(0)}, v^{(0)\prime}) - a_\varepsilon(\varepsilon^B, v^{(0)\prime}) + l_G(V) \tag{8}$$

where $\dot{(\cdot)}$ denotes the material derivative, and $(\cdot)'$ denotes shape derivative with respect to domain variation under a spatially fixed condition. The linear form $l_G(V)$ of the velocity function V is given by the following equations.

$$l_G(V) = \int_\Gamma G \nu_i V_i \, d\Gamma \tag{9}$$

$$G = -C_{ijkl} u_{k,l} v_{i,j} - \zeta C_{ijkl} u^{(0)}_{k,l} u_{m,i} v_{m,j} + C_{ijkl} u^{(0)}_{k,l} v^{(0)}_{i,j} - C_{ijkl} \varepsilon^B_{kl} v^{(0)}_{i,j} \tag{10}$$

where $\nu = \{\nu_i\}_{i=1,2,3}$ denotes the outward unit normal vector. From Eq. (8), the following optimality conditions with respect to u, v, $u^{(0)}$, $v^{(0)}$ are obtained.

$$a(u, v') + \zeta d(u^{(0)}, u, v') = 0 \quad \forall v' \in U \tag{11}$$

$$a(u', v) + \zeta d(u^{(0)}, u', v) = 0 \quad \forall u' \in U \tag{12}$$

$$d(u^{(0)}, u, v) = -1 \tag{13}$$

$$a(u^{(0)}, v^{(0)\prime}) = a_\varepsilon(\varepsilon^B, v^{(0)\prime}) \quad \forall v^{(0)\prime} \in U \tag{14}$$

$$a(u^{(0)\prime}, v^{(0)}) = \zeta d(u^{(0)\prime}, u, v) \quad \forall u^{(0)\prime} \in U \tag{15}$$

When $u^{(0)}$ and u are determined by Eqs. (2) and (3) respectively, Eqs. (11) and (14) are satisfied. Equations (12) and (15) are the adjoint equations to

determine the adjoint displacements v and $v^{(0)}$. Comparing Eqs.(11) and (12), the self-adjoint condition $u=v$ holds true for this problem. Equation (13) can be used for normalizing conditions to determine the magnitude of the eigen-mode u. When $u^{(0)}$, $v^{(0)}$, u and v are determined to satisfy Eqs.(11) to (15), the derivative of the Lagrange functional is expressed as follows.

$$\dot{L}=l_G(V) \tag{16}$$

From the fact that the vector function $G\nu$ is a coefficient function with respect to velocity V that is the derivation of the design function T_s, $G\nu$ indicates a sensitivity function of the buckling loading factor with respect to variation of each point on boundary in the outward normal direction. The sensitivity function is also called a shape gradient function. The scalar function G is the magnitude of the sensitivity and called the shape gradient density function.

3. Finite Element Model of Spine with Thoracic Cage

The spinal finite element model constructed in this study is shown in Fig. 1. This model consists of 6 cervical vertebrae, 12 thoracic vertebrae, 5 lumber vertebrae, intervertebral disks, intervertebral joints, 12 rib pairs, costovertebral articulations, costotransverse articulations, costicartilages, and sternum, excluding the atlas, sacrum, and coccyx. In this study, the muscle system supporting the spinal column remained out of consideration because instability resulting in a disorder is caused by a spinal deformity that the normal human muscle system cannot control. For geometrical shapes of spinal elements, commercial data of three-dimensional spine surface (Viewpoint Premier, catalog numbers of VP2886 and VP3611, Viewpoint Corporation, 498 7th Ave. Suite 1810, New York, NY 10018, USA) was used. Vertebrae were divided into about 40 subdomains respectively. The finite element meshes were made in their respective subdomains using a solid modeler (I-DEAS Master series version 2.1, SDRC, 2000 Eastman Drive, Milford, Ohio 45150-2789, USA) and combined. Manual modification was made to improve element qualities. The model comprises of 68,582 elements and 84,603 nodes, using hexahedral elements in 88% of the total elements, and pentahedral elements partially as well as a few tetrahedral elements. The element qualities are shown in Table 1.

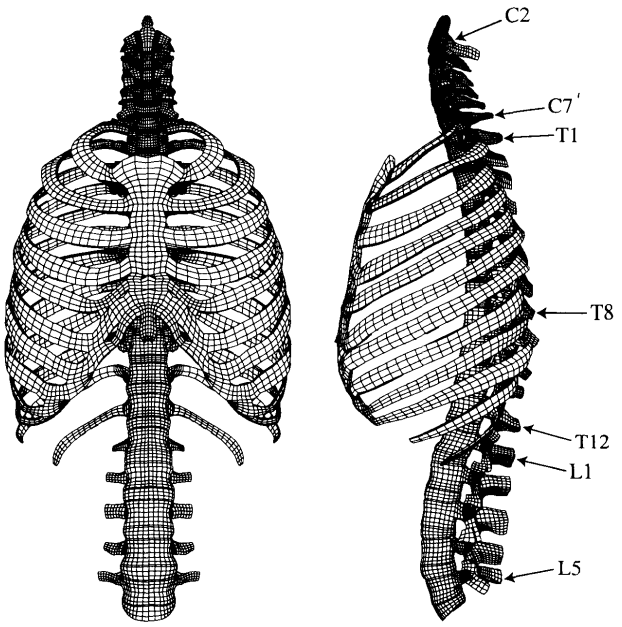

Fig. 1 Finite element model with thoracic cage

The aspect of the ninth and tenth thoracic vertebrae (T9 and T10) is shown in Fig. 2. Each vertebra consists of cancellous bone on the inside of the vertebral body and cortical bone on the surface of the vertebral body, vertebral arch, transverse process, spinal process and articular process. The intervertebral disks consist of nucleus pulposus in the center of the disks (approximately 60% of radius) and annulus fibrosus in the exterior of the disks. Adjacent vertebrae were connected with intervertebral disks and articular capsules of intervertebral joints. Costal bones and vertebrae are connected with costotransverse joint and costovertebral joint. Sternum and the costal bones form first to tenth are combined with costal cartilage.

The material properties of cortical bones and cancellous bones in vertebrae, ribs and sternum were assumed using the data by Yamada[6], since their materials are so hard that their material properties are insensitive to the spinal deformations. Material properties of intervertebral joints were identified by the experimental results of bending ligamentous cadaver spines devoid of musculature by Lucas and Bresler[7]. Young's modulus of intervertebral disks was determined by comparing with the reactions of the thoracic and lumber intervertebral disks to external forces of tension, compression and shearing in two directions and moments of bending in the two direc-

Table 1 Finite element qualities

Elements	Warping	Distortion	Stretch
Cortical bone Cancellous bone Costal cartilage	$< 43°$	> 0.6	> 0.05
Nucleus pulposus Anulus fibrosus Articular Costovertebral joint Costotransverse joint	$< 30°$	> 0.65	> 0.1

Table 2 Material properties

Elements (histology)	Young's modulus[MPa]	Poisson's ratio[-]
Cortical bone	17000	0.3
Cancellous bone	200	0.3
Nucleus pulposus	0.1	0.3
Anulus fibrosus	2.5*	0.3
Articular capsule (C2-T12)	7.5	0.3
Articular capsule (L1-L5)	0.6	0.3
Costovertebral joint	1.1	0.3
Costotransverse joint	1.1	0.3
Costal cartilage	500	0.3

*Shearing modulus is 5[MPa]

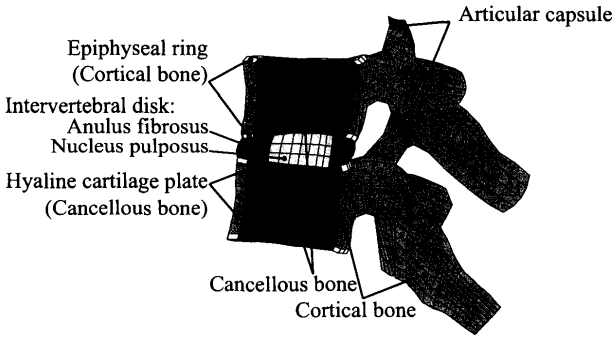

(a) Sagittal plane

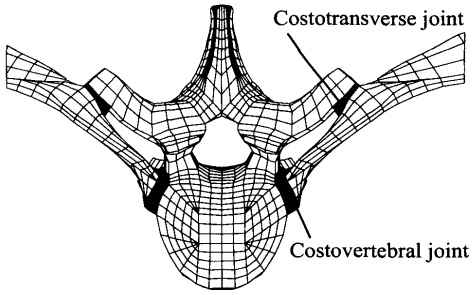

(b) Transverse plane

Fig. 2 Finite element mesh for the ninth and the tenth thoracic vertebrae

tions and torsion by Markolf[8]. Young's modulus of costovertebral articulations and costotransverse articulations were identified with the deformation properties of costosternal and costovertebral articulations when loading to ribs obtained by Schultz et al.[9] Table 2 shows the material properties of the spinal finite element model. Figure 3 shows comparison of stiffness for lateral bending between experimental results reported by Lucas and Bresler[7] and computed results with constructed finite element model removed the thoracic cage using a commercial finite element analysis program (MSC.Nastran version 7.0, MSC. Software Corporation, 815 Colorado Boulevard, Los Angeles, California 90041-1777, USA).

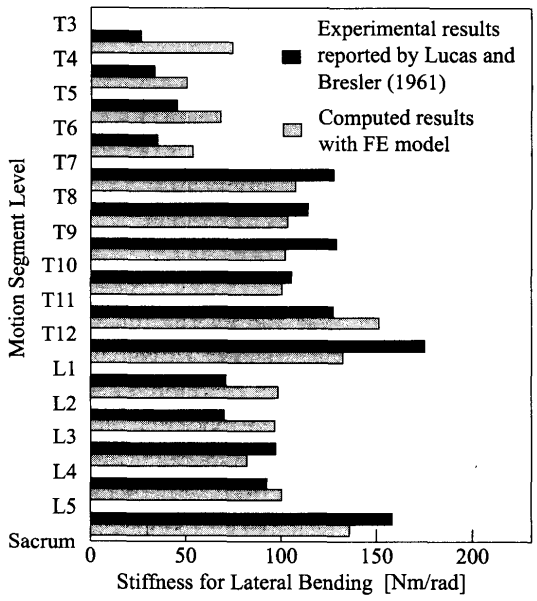

(a) With respect to segments

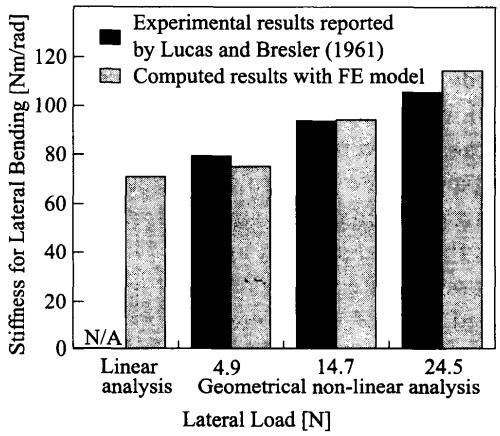

(b) With respect to loading levels

Fig. 3 Comparison of stiffness for lateral bending between experimental results reported by Lucas and Bresler[7] and computed results with constructed finite element model

4. Results of Buckling Analysis and Sensitivity Analysis

The prebuckling growth deformation $u^{(0)}$ was analyzed with generating initial strain (thermal strain) $\varepsilon^B = \bar{\varepsilon}^B \delta_{ij}$, where $\{\delta_{ij}\}_{i,j=1,2,3}$ is the Kronecker delta, on hyaline cartilage plate and epiphyseal ring of vertebrae from the fourth to the tenth (refer to Fig. 2). Displacement was fixed only on the adjacent surface with sacrum. Figure 4 shows the result of the fourth buckling mode analyzed with the prebuckling growth deformation that occurred at $\bar{\varepsilon}^B = 0.108$ which comes to vertebral body growth of 1.30% in length. The shape of the fourth buckling mode accorded with the clinical shape classified as the thoracic type as

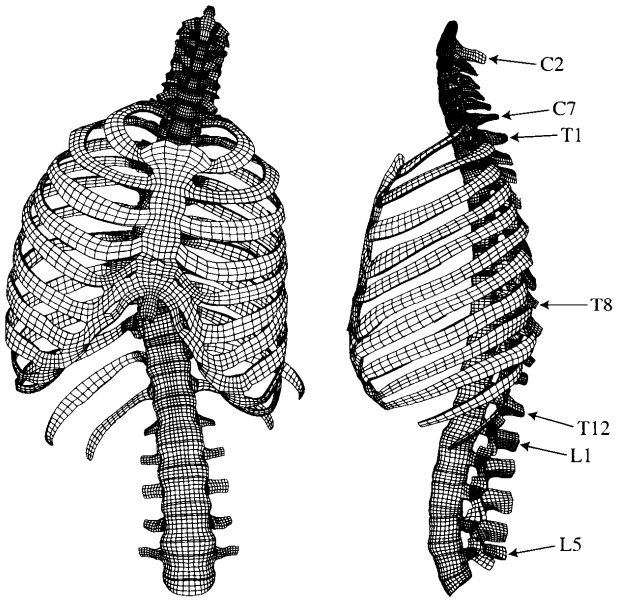

Fig. 4 Fourth buckling mode caused by growth of the fourth to the tenth vertebral bodies

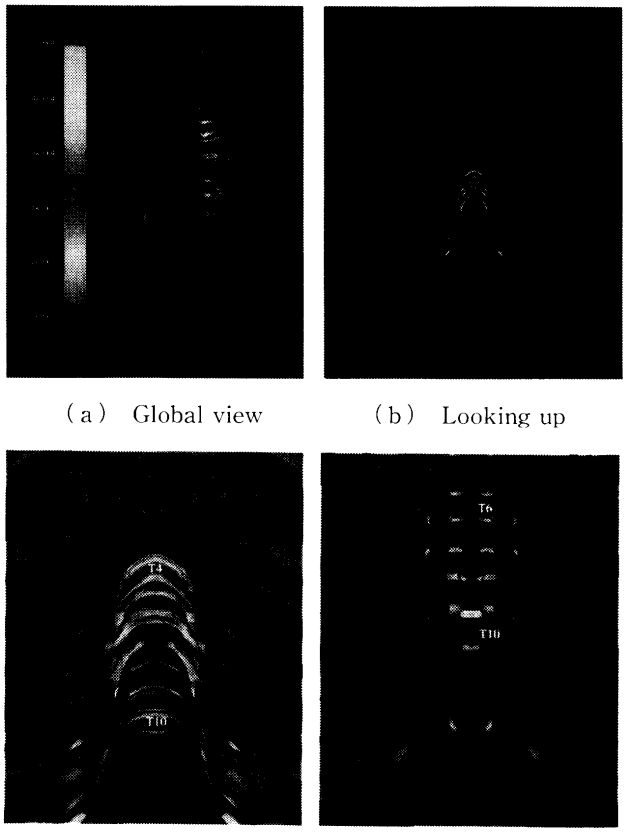

(a) Global view (b) Looking up

(c) Inside zoom (d) Rear zoom

Fig. 5 Distribution of shape gradient density function

shown in the previous paper[1].

Figure 5 shows the computational result of the shape gradient density function G with respect to maximization problem of buckling loading factor. The functions $u^{(0)}$, $v^{(0)}$, $u=v$, were evaluated based on

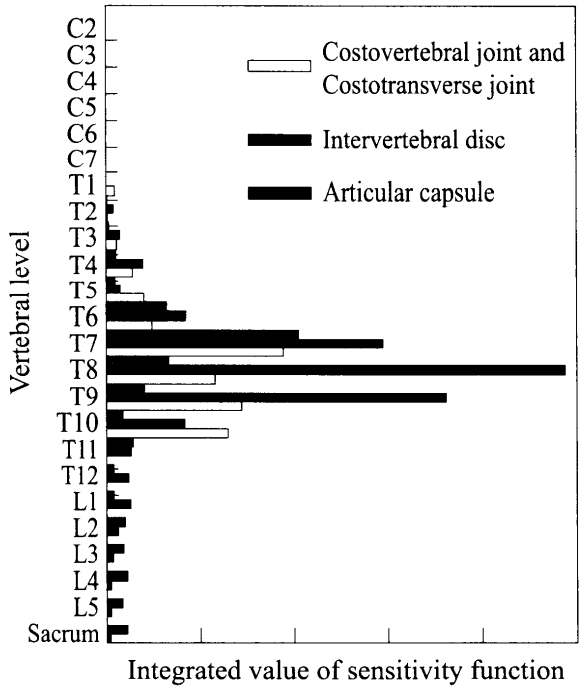

Fig. 6 Integrated values of shape gradient density function in each component of spine

Eqs. (14), (15), and (11) by a developed program using a commercial finite element analysis program (MSC. NASTRAN v. 70). The integrated values of G in each component of the spine are shown in Fig. 6.

5. Discussion

The shape gradient density function G evaluated by Eq. (10) has the meaning of the variational ratio of the fourth buckling loading factor with respect to variation of each point on boundary in the outward normal direction. The variation of boundary in the outward normal direction is accomplished by putting the same material of the spinal parts. Use of harder material with the same volume for the putting material on the boundary make the fourth buckling loading factor be greater.

If the fourth buckling hypothesis of the thoracic idiopathic scoliosis is acceptable and the growth part is correct for patients, the distribution map of G offers quantitative information for reinforcement with the same material on the boundary to correct the curvature and prevent the progression of the thoracic idiopathic scoliosis. Ordinary operative fusion treatments on vertebrae with screws and metallic rods realize more effective reinforcement than that with living tissue. The reasonable selection of the fusion vertebrae can minimize fusion area.

The result shown in Figs. 5 and 6 illustrates that the shape gradient density function G is high at the articular capsules of the intervertebral joints, the

intervertebral disks, the costotransverse joints and the costovertebral joints between the sixth and the eighth thoracic vertebrae where the apex of the curvature in the case of the thoracic idiopathic scoliosis appears. This result suggests that fusion treatments on the neighborhood of the apex are most effective to correct the curvature and to prevent the progression.

6. Conclusion

Based on the fourth buckling hypothesis induced by the growth of thoracic vertebral bodies concerning the mechanical etiology of the thoracic idiopathic scoliosis, this paper presents a theory and numerical results on the sensitivity function with respect to the critical growth of thoracic vertebrae on the maximization problem of the fourth buckling load. The numerical results analyzed by the finite element method demonstrated that the shape gradient function is high at the articular capsules of the intervertebral joints, the intervertebral disks, the costotransverse joints and the costovertebral joints between the sixth and the eighth thoracic vertebrae where the apex of the curvature in the case of the thoracic idiopathic scoliosis appears.

This study was supported by a Grant-in-Aid for Scientific Research (B) of Japan Society for the Promotion of Science (No. 12450047).

References

(1) Azegami, H., Murachi, S., Kitoh, J., Ishida, Y., Kawakami, N. and Makino, M., Etiology of Idiopathic Scoliosis: Computational Study, Clinical Orthopaedics and Related Research, No. 357 (1998), pp. 229-236.

(2) Azegami, H., Shimoda, M., Katamine, E. and Wu, Z.C., A Domain Optimization Technique for Elliptic Boundary Value Problems, Hernandez, S., El-Sayed, M. and Brebbia, C.A., eds., Computer Aided Optimization Design of Structures IV, Structural Optimization (1995), pp. 51-58, Computational Mechanics Publications, Southampton.

(3) Azegami, H. and Wu, Z.C., Domain Optimization Analysis in Linear Elastic Problems (Approach Using Traction Method), JSME Int. J. Ser. A, Vol. 39, No. 2 (1996), pp. 272-278.

(4) Azegami, H., Kaizu, S., Shimoda, M. and Katamine, E., Irregularity of Shape Optimization Problems and an Improvement Technique, Hernandez, S. and Brebbia, C.A., eds., Computer Aided Optimization Design of Structures V (1997), pp. 309-326, Computational Mechanics Publications, Southampton.

(5) Azegami, H., Sugai, Y. and Shimoda, M., Shape Optimization with Respect to Buckling, Hernandez, S., Kassab, J. and Brebbia, C.A., eds., Computer Aided Optimization Design of Structures VI (1999), pp. 57-66, WIT Press, Southampton.

(6) Yamada, H., Strength of Biological Materials (1970), pp. 19-104, The Williams & Wilkins Company.

(7) Lucas, D.B. and Bresler, B., Stability of the Ligamentous Spine, Biomechanics Laboratory Rpt. 40 (1961), Univ. of California.

(8) Markolf, K.L., Deformation of the Thoracolumbar Interbertebral Joints in Response to External Loads, J. Bone and Joint Surg., Vol. 54A (1972), pp. 511-533.

(9) Schultz, A.B., Benson, D.R. and Hirsch, C., Force Deformation Properties of Human Cost-sternal and Cost-vertebral Articulations, J. Biomechanics, Vol. 7 (1974), pp. 311-318.